SLAC-PUB-5667
August 1991
T/E

Perturbation Theory In Light-Cone Quantization*

ALEX LANGNAU‡ AND STANLEY J. BRODSKY

Stanford Linear Accelerator Center

Stanford University, Stanford, California 94309

ABSTRACT

A new algorithm for the automatic computation of Feynman diagram amplitudes in quantum field theory is presented. Once the topology of a diagram is defined, the algorithm constructs all corresponding light-cone time-orderings. We explore the method for two- and three-loop calculations in QED.

Submitted to Journal of Computational Physics

* Supported in part by the Department of energy under contract DE-AC03-76SF00515.
‡ Supported in part by a grant from Studienstiftung des deutschen Volkes.

1. Introduction

Feynman perturbation theory has become the most practical tool for computing cross sections in high energy physics and other physical properties of field theory. Although this standard covariant method has been applied to a great range of problems, computations beyond one-loop corrections are very difficult. A number of examples of two-loop and higher calculations using Feynman methods are given in Ref. [1].

Because of the algebraic complexity of the Feynman calculations in higher-order perturbation theory, it is desirable to automatize Feynman diagram calculations so that algebraic manipulation programs can carry out almost the entire calculation. This paper presents a step in this direction. The technique we are elaborating on here is known as light-cone perturbation theory (LCPTh) [2,3,4].

LCPTh is similar to ordinary time-ordered perturbation theory, familiar in both non-relativistic quantum mechanics and quantum field theory, where each time-ordered amplitude is constructed from a product of energy denominators and interaction vertices. The covariant Feynman amplitude is, in principle, obtained from the sum of time-ordered non-covariant graphs with the same topology. Instead of ordinary time, the LCPTh evolution parameter is the time along the light-cone $\tau = t - z/c$. The $\tau-$ ordered amplitudes are each invariant under a large class of Lorentz boosts, so that each $\tau-$ordered amplitude is itself frame-independent with respect to those symmetries.

A straightforward way of relating the LCPTh amplitudes to the Feynman rules is by changing variables of the independent loop momenta k in a Feynman integral according to [5, 6]

$$\int d^4k \to \frac{1}{2}\int dk^+ d^2k_\perp dk^-$$

with $k^\pm = k^0 \pm k^3$, and performing the integration over k^-. The residues give the LCPTh amplitudes. Alternatively, these amplitudes can be obtained directly from the Hamiltonian formalism derived at fixed τ. Thus by constructing LCPTh directly, only a three dimensional integral has to be performed for each loop. Since the complex contour integrations over energy or k^- do not occur, the formalism is immediately suitable for numerical treatment.

The price to pay for the simple features of LCPTh is that every Feynman diagram with n vertices gets decomposed into a set of light-cone time-ordered diagrams. However, unlike time-ordered perturbation theory (which can be obtained after performing the k^0 integration of the independent loop momenta), the number of light-cone time-orderings corresponding to the Feynman amplitude is considerably smaller than n! For example, in the case of the fourth order $(\frac{\alpha}{\pi})^2$ correction to the electron's anomalous moment (without vacuum polarization), there are 516 individual time-ordered contributions, but only 8 of them are non-vanishing in the light-cone formalism. This example will be discussed further in the following sections.

There are a number of other advantages of the light-cone perturbation theory formalism.

- Since each amplitude describes the propagation of on-mass-shell particles with a specific time-ordering, the physical meaning of each LCPTh amplitude is immediate. General properties such as unitarity and cluster decomposition theorems become explicit.

- If one quantizes in a physical gauge, all intermediate states correspond to the propagation of physical particles with positive metric. The physical variables used to describe jets or particles in high energy physics have an immediate interpretation in terms of the LC variables.
- The cancellation of infrared divergences is immediate and can be carried out for contributions with the same LC time-ordering.
- The LC quantization of quantum chromodynamics leads to a direct physical interpretation of the theory. The implementation of current algebra becomes essentially a kinematic problem [7,8,9]. The current matrix elements J^+ needed to compute form factors and structure functions can be written as diagonal matrix elements of the light-cone wavefunctions, since such currents do not couple to vacuum fluctuations in the LC quantized theory [9].

[10] .

Recently light-cone quantized field theories have been investigated in the context of developing non-perturbative methods for the solution of field theories [10]. An outstanding problem confronting these non-perturbative Hamiltonian approaches to quantum field theory is the implementation of ultraviolet regularization and covariant renormalization [11]. A necessary first step for solving these problems is to validate the renormalization methods at the perturbative level. LCPTh thus serves as an essential testing ground for these studies.

2. A general algorithm for generating LCPTh

In this section we develop a procedure which automatically constructs all light-cone time-orderings associated with a given Feynman diagram F. The only input required is the set of photon connections of F (first photon (4,1), second photon (5,2) in Fig. 1), which define the topology of the diagram.

In the first part of this section we outline the procedure for quantum electrodynamics in the specific example of Fig. 1. In the remainder of the section a general algorithm, useful for higher loop calculations, is described.

First we shall review a procedure introduced by Soper [2]. The Feynman answer F for the two-loop contribution to the electromagnetic vertex $\gamma^*(q) + e^-_\downarrow(p_I) \rightarrow e^-_\uparrow(p_F)$ corresponding to Fig. 1 is given by [9,12]

$$\begin{aligned} F = e^4 \int & d^4x_1 d^4x_2 d^4x_3 d^4x_4 d^4x_5 \overline{\Psi}(x_5,\uparrow)\gamma^\mu \\ & \times iS_F(x_5-x_4)\gamma^\lambda iS_F(x_4-x_3)\frac{\gamma^+ e^{-iqx_3}}{p_I^+} iS_F(x_3-x_2)\gamma^\nu \\ & \times iS_F(x_2-x_1))\gamma^\rho \Psi(x_1,\downarrow) \quad iD_{F,\lambda\rho}(x_4-x_1) iD_{F,\mu\nu}(x_5-x_2)\ , \end{aligned} \tag{2.1}$$

where p_I^+ denotes the incoming light-cone momentum of the electron. Here we have chosen the helicity-flip amplitude $\left\langle p_F|\frac{J^+}{p_I^+}|p_I\right\rangle$ and the frame with $q^+ = 0$ which is appropriate for obtaining the anomalous magnetic moment of the electron and its Pauli form factor $F_2(q^2)$ [13] . The Feynman propagator can be written in the convenient form [3]

$$S_F(x) = \frac{-i}{(2\pi)^3}\int d^2p_\perp \int_0^\infty \frac{dp^+}{p^+}\left(\Theta(x^+)(\not{p}+m)e^{-ipx} + \Theta(-x^+)(-\not{p}+m)e^{ipx}\right)$$
$$+ \frac{1}{(2\pi)^3}\delta(x^+)\frac{1}{2}\gamma^+\int d^2p_\perp \int_0^\infty \frac{dp^+}{p^+}e^{-i(\frac{1}{2}p^+x^- - p_\perp x_\perp)}$$
$$= S_F^{(+)}(x) + S_F^{(-)}(x) + S_F^{Inst.}(x)\ , \tag{2.2}$$

where the electron four-vector is on the mass shell *i.e.* $p^- = \frac{m^2+p_\perp^2}{p^+}$. This result follows from

$$S_F(x) = (i\partial_\mu\gamma^\mu + m)\Delta_F(x) \tag{2.3}$$

and

$$\Delta_F(x) = \frac{-i}{(2\pi)^3}\int d^2p_\perp \int_0^\infty \frac{dp^+}{p^+}\left(\Theta(x^+)e^{-ipx} + \Theta(-x^+)e^{ipx}\right).$$

The third term in Eq. (2.2) gives rise to an instantaneous fermion interaction in light-cone quantized QED. The photon propagator in light-cone gauge $\eta\cdot A = A^+ = 0$ is given by

$$D_{\mu\nu}(x) = \frac{-i}{(2\pi)^3}\int d^2k_\perp \int_0^\infty \frac{dk^+}{k^+}\left(e^{-ikx}\Theta(x^+) + e^{ikx}\Theta(-x^+)\right)\sum_\lambda \epsilon_\mu^*(k,\lambda)\epsilon_\nu(k,\lambda)$$
$$+ \int d^2k_\perp \int_0^\infty dk^+\delta(x^+)\frac{2}{(2\pi)^3}\delta_{\mu+}\delta_{\nu+}\frac{1}{k^{+2}}e^{-i(\frac{1}{2}k^+x^- - k_\perp x_\perp)}$$
$$\equiv D_{\mu\nu}^{(+)}(x) + D_{\mu\nu}^{(-)}(x) + D_{\mu\nu}^{Inst.}(x) \tag{2.4}$$

where

$$\sum_{\lambda=1,2}\epsilon_\mu^*(k,\lambda)\epsilon_\nu(k,\lambda) = -g_{\mu\nu} + \frac{\eta_\mu k_\nu + \eta_\nu k_\mu}{\eta k}\ .$$

This result can be obtained by performing the k^- integration of

$$D_{\mu\nu}(x) = \frac{1}{(2\pi)^4} \int d^4k e^{-ikx} \frac{-g_{\mu\nu}}{k^2 + i\epsilon}. \tag{2.5}$$

The external field Ψ_I for the incident electron is given by

$$\Psi_I(x) = u_I(p,s) e^{-ip_I x} \tag{2.6}$$

where $u_I(p,s)$ is the solution of the free Dirac equation. In Feynman gauge the polarization sum $\sum_{\lambda=1,2} \epsilon^*_\mu(k,\lambda)\epsilon_\nu(k,\lambda)$ in (2.4) gets replaced by $-g_{\mu\nu}$ and the instantaneous contribution drops out.

In order to compute the scattering amplitude, Eq. (2.1), using light-cone perturbation theory, one first has to split up the integration region into all possible time-orderings. For illustration purposes we pick a typical time-ordering τ_{14325}

$$x_1^+ < x_4^+ < x_3^+ < x_2^+ < x_5^+ \tag{2.7}$$

and obtain the contribution

$$\begin{aligned} F^{(\tau)}_{(14325)} = e^4 \int & d^4x_1 d^4x_2 d^4x_3 d^4x_4 d^4x_5 \\ & \times \Theta(x_4^+ - x_1^+)\Theta(x_3^+ - x_4^+)\Theta(x_2^+ - x_3^+)\Theta(x_5^+ - x_2^+)\; e^{+ip_F x_5} \overline{u}(p_F,\uparrow)\gamma^\mu \\ & \times iS_F^{(+)}(x_5 - x_4)\gamma^\lambda\, iS_F^{(-)}(x_4 - x_3)\; \frac{\gamma^+ e^{-iqx_3}}{p_I^+}\; iS_F^{(-)}(x_3 - x_2)\gamma^\nu \\ & \times iS_F^{(+)}(x_2 - x_1)(\gamma^\rho e^{-ip_I x_1} u(p_I,\downarrow))\, iD^{(+)}_{F,\lambda\rho}(x_4 - x_1)\, iD^{(+)}_{F,\mu\nu}(x_5 - x_2)\;. \end{aligned} \tag{2.8}$$

The corresponding τ-ordered diagram is shown in Fig. 2. Note that the instantaneous contributions in $S_F(x_4 - x_3)$ and $S_F(x_3 - x_2)$ do not contribute because of

$\gamma^+\gamma^+ = 0$. The instantaneous contribution of $S_F(x_2 - x_1)$ gives zero result in this case due to

$$\delta(x_2^+ - x_1^+)\Theta(x_4^+ - x_1^+)\Theta(x_3^+ - x_4^+)\Theta(x_2^+ - x_3^+)\Theta(x_5^+ - x_2^+) \equiv 0.$$

In the same way it is shown that the instantaneous contribution of $S_F(x_5 - x_4)$ vanishes. In general, instantaneous interactions give rise to a nonzero contribution only if they do not extend over more than one intermediate state for the same reason [5]. Eq. (2.8) leads to a phase factor of the form

$$\begin{aligned} &\exp\{i\,[p_F x_5 - p_4(x_5 - x_4) + p_3(x_4 - x_3) + p_2(x_3 - x_2) \\ &-qx_3 - p_1(x_2 - x_1) - p_I x_1 - k_1(x_4 - x_1) - k_2(x_5 - x_2)]\}\ . \end{aligned} \tag{2.9}$$

The momenta p_i, k_j denote the momentum associated with the i-th fermion and the j-th photon line respectively. The momenta p_I, p_F corresponds to the initial and final momentum respectively. The integration over $x_i^\perp, x_i^-$ can be performed trivially and demonstrates momentum conservation of $p_i^+, p_i^\perp$ at each vertex.

In order to perform the x_i^+ integration, it is convenient to change variables according to [2]

$$\begin{aligned} \lambda_1^+ &= x_4^+ - x_1^+ \\ \lambda_2^+ &= x_3^+ - x_4^+ \\ \lambda_3^+ &= x_2^+ - x_3^+ \\ \lambda_4^+ &= x_5^+ - x_2^+\ . \end{aligned} \tag{2.10}$$

The light-cone time part of Equation (2.9) becomes

$$\begin{aligned} &\exp\tfrac{1}{2}\left[i\lambda_4^+\left(p_4^- - k_2^- - p_F^-\right) + i\lambda_3^+\left(-p_2^- - p_1^- - p_4^- + p_F^-\right)\right. \\ &\left. + i\lambda_2^+\left(-p_3^- - p_1^- - p_4^- + p_F^- - q^-\right) + i\lambda_1^+\left(-k_1^- - p_1^- + p_F^- - q^-\right) + ix_1^+\left(-p_I^- - q^- + p_F^-\right)\right] \\ &= \exp\tfrac{1}{2}\left[iC_F(\tau_{14325}) + ix_1^+\left(-p_I^- - q^- + p_F^-\right)\right]\ , \end{aligned} \tag{2.11}$$

This will play an important role in our discussion, so we have introduced the definition of a characteristic exponent $C_F(\tau)$ of a time-ordering τ. The integral over x_1^+ can be performed trivially and gives overall light-cone energy conservation. The remaining integrals over x_i^+ can be performed by means of

$$\int_0^\infty dT e^{i(H+i\epsilon)T} = \frac{i}{H+i\epsilon} .$$

The product of these denominators, and the factors $\frac{-i}{(2\pi)^3}\frac{1}{p^+}$ from (2.2) and (2.4) then lead to the LCPTh answer of the time-ordering (2.7).

As far as the treatment of instantaneous diagrams is concerned, a simple substitution allows the incorporation of instantaneous vertices [5]. To see this, consider the γ^+ contribution of one fermion line to an arbitrary Feynman diagram

$$F = \ldots \left(\frac{\frac{1}{2}\gamma^+ p^-}{p^+ d^-} + \frac{\gamma^+}{2p^+} \right) \ldots , \tag{2.12}$$

where $d^- = p_I^- - p^- - \sum_{\text{spec}} p_i^-$ is the light-cone denominator containing the fermion line under consideration. In general, p_I^- is given by the total light-cone energy of the incoming particles and the sum runs over all spectators of the corresponding intermediate state.

The second term in Eq. (2.12) presents the instantaneous contribution to F. If we define $p^-_{\text{energy-shell}} = p^- + d^-$, both terms combine to

$$F = \ldots \frac{\frac{1}{2}\gamma^+ p^-_{\text{energy-shell}}}{p^+ d^-} \ldots . \tag{2.13}$$

Note that $p^-_{\text{energy-shell}}$ is the light-cone energy one would obtain if one required light-cone energy conservation at the vertex. Thus all instantaneous fermion contributions can be taken into account by putting those p^- on energy-shell in the

numerator whenever that fermion does not extend over more than one intermediate state [5]. In the same way the light-cone gauge photon interaction in (2.4) can be handled [4].

Now we are ready to describe our general as a sequence of 10 steps (see Fig. 3). For illustration we again consider the order e^5 contribution to the electron vertex. We start out noting that each two-loop τ-ordered contribution to the electron vertex (which contains no vacuum polarization contribution [14]) is of the form

$$F(i_1,\ldots,i_5) = \frac{e^4}{(16\pi^3)^2}\int \frac{dk_1^+ d^2k_1 dk_2^+ d^2k_2}{p_1^+ p_2^+ p_3^+ p_4^+ k_1^+ k_2^+}\ \frac{\Theta(p_1^+)\Theta(p_2^+)\Theta(p_3^+)\Theta(p_4^+)}{d^-(1)d^-(2)d^-(3)d^-(4)}$$
$$\times \Big(\overline{u}\gamma^{\mu(i_1)}(s_4\not{p}_4+m)\gamma^{\mu(i_2)}(s_3\not{p}_3+m)\gamma^{\mu(i_3)}(s_2\not{p}_2+m)\gamma^{\mu(i_4)}$$
$$\times\ (s_1\not{p}_1+m)\gamma^{\mu(i_5)}u\Big)\quad D_{\mu(1)\mu(2)}(k_1)\,D_{\mu(4)\mu(5)}(k_2) \tag{2.14}$$

where the diagram is defined by its photon connections. The explicit construction of (2.14) is done as follows:

- Step (I): the indices $i_1, i_2, ..., i_5$ are specified. For the diagram of Fig. 1 we have $i_1 = 5, i_2 = 2, i_3 = +, i_4 = 4, i_5 = 1$. For the diagram of Fig. 4 we have $i_1 = 5, i_2 = +, i_3 = 2, i_4 = 4, i_5 = 1$.

- Step (II): For each of the $n! = 120$ time-orderings one defines a vector $\tau(I), i = 1, ..., n = 5$. $\tau(I)$ describes the position of the I-th vertex of F. In the example of Fig. 1 we get $\tau(1) = 1, \tau(2) = 2, \tau(3) = 3, \tau(4) = 4, \tau(5) = 5$. In the example of Fig. 2 we get $\tau(1) = 1, \tau(2) = 4, \tau(3) = 3, \tau(4) = 2, \tau(5) = 5$. It is also useful to define

$$A(\tau(I)) = I\ . \tag{2.15}$$

- Step (III): Once a time-ordering is defined we know which pieces out of

the propagators (2.2) and (2.4) are to be picked. The construction of $C_F(\tau)$ defined in (2.9) is straightforward. Note that the term which describes overall momentum conservation must be subtracted in order to obtain $C_F(\tau)$.

- Step (IV): one changes variables to $\lambda_k^+ = x_{i_{k+1}}^+ - x_{i_k}^+$ for $k = 1, ..., 4$ and expresses the characteristic exponential in terms of λ_k

$$C_F(\tau) = \sum_i \lambda_i^+ d^-(i) \; .$$

- Step (V): In general 5! different time-orderings can contribute to F. However, in practice most of them vanish. This is due to the fact that all light-cone momenta are greater or equal zero and conserved at each vertex [15] . An example is given in Fig. 5, which contains a vacuum fluctuation at x_4. A vacuum fluctuation at x_i can be formally identified when all terms of $d^-(i)$ carry the same coefficient (namely $+1$, or -1). The $d^-(i)$ can be obtained from $C_F(\tau)$ by setting $\lambda_k = \delta_{ki}$.

- Step (VI): To obtain the form Eq. (2.14) all momenta p_i^+ and $p_i^\perp$ must be expressed in terms of the independent loop momenta and external momenta. This can be achieved by solving the equations

$$\begin{aligned} d^-(1) &= 0, \\ d^-(2) &= 0, \\ d^-(3) &= 0, \\ d^-(4) &= 0 \; . \end{aligned} \tag{2.16}$$

For example, for Fig. 2 we find

$$p_1^+ = p_I^+ - k_1^+, \quad p_{1\perp} = p_{I\perp} - k_{1\perp}$$

$$p_2^+ = k_1^+ + k_2^+ - p_I^+, \quad p_{2\perp} = k_{1\perp} + k_{2\perp} - p_{I\perp}$$

$$p_3^+ = k_2^+ + k_1^+ - p_F^+, \quad p_{3\perp} = k_{2\perp} + k_{1\perp} - p_{F\perp}$$

$$p_4^+ = -k_2^+ + p_F^+, \quad p_{4\perp} = -k_{2\perp} + p_{F\perp} \; . \tag{2.17}$$

- Step (VII): The expressions for the internal fermion momenta, obtained in step (VI), are substituted into $d^-(i)$ in order to construct all energy denominators $d^-(i)$ explicitly.
- Step (VIII): When setting up the fermion p_i^- in the numerator it must be decided whether the fermion line p_i extends over more than one intermediate state. A formal criteria for that is given by

$$abs(A(i) - A(i+1)) = 1 \; . \tag{2.18}$$

  If (2.18) is correct, p_i^- is set on energy shell, which means

$$p_i^- = p_{i,\text{mass-shell}} + d^-(ins) \tag{2.19}$$

  where $ins := \min(A(i+1), A(i)), p_{i,\text{mass-shell}}^- = \frac{m^2+p_{i\perp}^2}{p_i^+}$. If (2.18) is not fulfilled we have $p_i^- = p_{i,\text{mass-shell}}^-$.
- Step (IX). The only variables which are left to be determined in (2.14) are the signs s_i which define whether a fermion or antifermion propagates. The phase can be determined from

$$s_i = \frac{A(x_{i+1}) - A(x_i)}{abs\,(A(x_{i+1}) - A(x_i))} \; . \tag{2.20}$$

- Step (X): (2.14) can now be calculated. If necessary, the diagram can be regularized using Pauli-Villars regularization.

It should be noted that step 2 to step 10 can be readily carried out automatically, using an algebraic manipulation program like REDUCE. The algorithm can be generalized easily to higher loops. As an example, in Fig. 6 we present the time-orderings, generated by the algorithm, to a three-loop contribution of the electromagnetic vertex for $q^+ = 0$.

3. Numerical Results

In this section we report on the use of the general LCPTh algorithm to redo the two-loop calculation of the anomalous magnetic moment $\frac{g-2}{2} = a = F_2(0)$ by Petermann and Sommerfield [16,17]. Figure 7 shows all Feynman diagrams as well as the corresponding light-cone time-orderings, contributing to the anomaly in fourth order.

The vacuum polarization diagram 6 can be computed by the effective replacement [18]

$$\frac{1}{k^2 - \lambda^2 + i\epsilon} \rightarrow \frac{\alpha}{\pi} \int_0^1 dt \, \frac{t^2(1 - \frac{1}{3}t^2)}{1 - t^2} \, \frac{1}{k^2 - \frac{4m_e^2}{1-t^2} + i\epsilon} \tag{3.1}$$

after performing the integration over k^- [19,20], All diagrams in Fig. 7 (with exception of graph 5) are ultraviolet divergent and require renormalization. However, by computing certain sets of diagrams simultaneously, the calculation can be arranged such that ultraviolet divergences cancel between diagrams of the same set. As an example, Table I shows the result of the numerical integration, using the adaptive integration routine VEGAS [21]. of diagram 1 and 2 for different values for the ultraviolet cut off Λ^2. After mass renormalization of the self-energy

diagram 2, we observe only a residual Λ dependence of the form

$$\frac{1}{\Lambda^2}\log\Lambda^2 \tag{3.2}$$

which can be easily eliminated by an appropriate fit in Λ^2 [22].

We obtain for our estimate of diagram 1 and 2, $a = -0.326 \pm 0.001\frac{\alpha^2}{\pi^2}$, which is to be compared with the analytic answer of Petermann [23] $a = -0.327\ldots\frac{\alpha^2}{\pi^2}$ and Sommerfield. Table II shows the result of the residual diagrams. The agreement with the correct result is better than 0.2% To obtain these results we needed typically only one minute of CPU per graph on a IBM3090. These successes encouraged us to attempt some sixth order moment calculations for the Feynman graphs shown in Fig. 8. In Table III we compare our estimate with the results obtained by Brodsky and Kinoshita [24]. For further references see also [25] .

4. Summary

We have presented a new algorithm for the automatic computation of Feynman diagram amplitudes. The method, which is based on light-cone perturbation theory (LCPTh), is explored for two- and three-loop calculations in QED. The amplitudes are constructed automatically and explicitly, given just the photon connections of the corresponding diagrams. The extension of the algorithm to higher loops is straightforward [26] .

One of the most useful applications of LCPTh and this algorithm could be the computation of multi-jet processes in e^+e^-− annihilation, since LCPTh amplitudes correspond closely to the quark and gluon jets identified in high energy physics. These reactions have not been completely calculated beyond the one-loop

order in perturbation theory. However, the extension to quantum chromodynamics requires a more careful regularization of the ultraviolet behavior of the theory. The implementation of dimensional regularization and other renormalization issues are described elsewhere [27] .

Acknowledgements

We would like to thank J. Taron and M. Burkardt for helpful comments. One of us (A.L.) would like to acknowledge Mountaz Zizi for her constructive suggestions concerning certain techniques which turned out to be essential for this work.

FIGURE CAPTIONS

1) Two-loop QED cross diagram. The momenta p_i and k_j correspond to the internal momenta of the i-th fermion and j-th photon respectively.

2) Light-cone time-ordering contributing to the cross diagram.

3) Flow chart for the automatic computation of QED amplitudes.

4) Two-loop "corner" diagram.

5) Example for a vacuum fluctuation to the cross diagram.

6) Example for a set of light-cone time-orderings which correspond to a sixth order Feynman diagram.

7) Six Feynman diagrams and the corresponding light-cone time-orderings contributing to the fourth order anomalous magnetic moment to the electron.

8) Sixth-order Feynman diagrams containing one-loop vacuum polarization.

TABLE CAPTIONS

1: Result (δa) of the numerical integration for diagram $1 + 2$ after mass renormalization in units of $(\frac{\alpha^2}{\pi})^2$. The data converge for large values of the Pauli-Villars cut-off Λ (in units of the electron mass).

2: Numerical results (δa) for the two-loop diagrams of Fig. 7. The results are compared with the analytic answer by Petermann.

3: Numerical results (δa) for the sixth-order contributions of the diagrams in Fig. 8. The results are compared with the results given by Brodsky and Kinoshita.

REFERENCES

[1] Kinoshita, T., Quantum Electrodynamics. N.J., World Scientific, 1990; T. Kinoshita, B. Nizic, Y. Okamoto, Phys. Rev D41, 593 (1990); S. G. Gorishny, A. L. Kataev, and S. A. Larin, Phys.Lett. B212, 238 (1988).

[2] David E. Soper, SLAC-PUB-0137 (1971).

[3] John B. Kogut, Davison E. Soper, Phys. Rev. D1, 2901 (1970).

[4] G. P. Lepage and S. J. Brodsky, Phys. Rev. D22, 2157 (1980).

[5] S. J. Brodsky, R. Roskies and R. Suaya, Phys. Rev. D8, 4574 (1973).

[6] M. G. Schmidt, Phys. Rev. D9, 408 (1974).

[7] Y. Frishman, Phys. Reports 13C, 1 (1974).

[8] J. D. Bjorken, J. B. Kogut and D. E. Soper, Phys. Rev. D3, 1382 (1971).

[9] S. D. Drell, D. J. Levy, and T. M. Yan, Phys. Rev. Lett. 22, 744 (1969); Phys. Rev. 187, 2159 (1969).

[10] H. C. Pauli and S. J. Brodsky, Phys. Rev. D32, 1993 (1987); 2001 (1987); T. Eller, H.-C. Pauli and S. J. Brodsky, Phys. Rev. D35, 1493 (1987); K. Hornbostel, Ph.D. Thesis, SLAC REPORT No. 0333 (1989) ; M. Burkardt, Nucl. Phys. A504, 762 (1989); R. J. Perry, A. Harindranath and K. G. Wilson, Phys. Rev. Lett. 65, 2959 (1990); R. J. Perry, A. Harindranath, Phys. Rev. D43, 492 (1991); R. J. Perry, A. Harindranath, Phys. Rev. D43, 4051 (1991).

[11] P. Griffin, Fermilab-Pub-91/197-T.

[12] More precisely the spin-flip amplitude of the γ^+ current with momentum transfer $(0, 0, q_x, q_y)$ projects out $(q_x + iq_y)F_2(0)$.

[13] S. J. Brodsky, S. D. Drell, Phys. Rev. D22, 2236 (1980)

[14] The vacuum polarization diagram can be taken into account by a similar expression to Eq. (2.14) (at one loop) where the photon propagator is replaced by an effective one loop propagator. We will discuss this point in the next section.

[15] This is one of the main advantages of x^+-ordered perturbation theory.

[16] A. Petermann, Helv. Phys. Acta 30, 407 (1957)

[17] C. M. Sommerfield, Ann. Phys.(N.Y.) 5, 26 (1958).

[18] G.Kallen, Hel. Phys. Acta 25, 417 (1952).

[19] This is why only one time-ordering appears for this graph.

[20] The same can be done for two loop vacuum polarization insertions.

[21] G. P. Lepage, J. Comput. Phys. D27, 192 (1978).

[22] The mass renormalization can be performed in this case by the method of alternate denominators. [5] Whenever one Fock state appears twice in a diagram, the total energy which appears in the denominator(s) of the embedded self-energy must be replaced by the total energy adjacent to this self-energy correction In order to keep the discussion as simple as possible, we have not included this step into the logic of Fig. 5. However, this can be done in a straightforward way, when ultraviolet regularization is needed.

[23] A. Petermann, Helv. Phys. Acta 30, 407 (1957).

[24] S. Brodsky and T. Kinoshita, Phys. Rev. D3, 356 (1971).

[25] T. Kinoshita, B. Nizic, Y. Okamoto, Phys. Rev D41, 593 (1990)

[26] However, the numerical effort, necessary to obtain stable and reliable results, typically increases by one order of magnitude, at each increasing order in perturbation theory.

[27] A. Langnau, Ph.D Thesis in preparation.

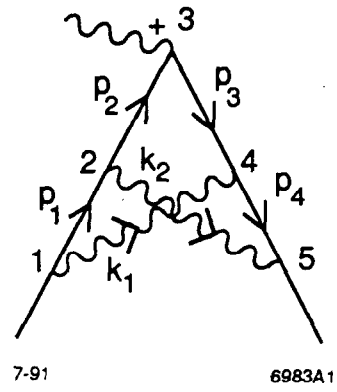
3
p2
p3
2
k2
4
p4
p1
1
k1
5
7-91
6983A1

Fig. 1

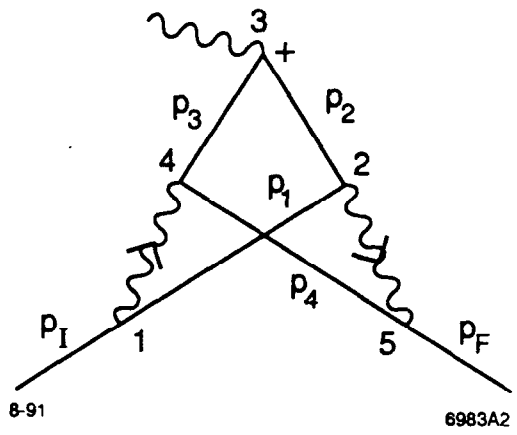
3
p3
p2
4
2
p1
p4
pI
1
5
pF
8-91
6983A2

Fig. 2

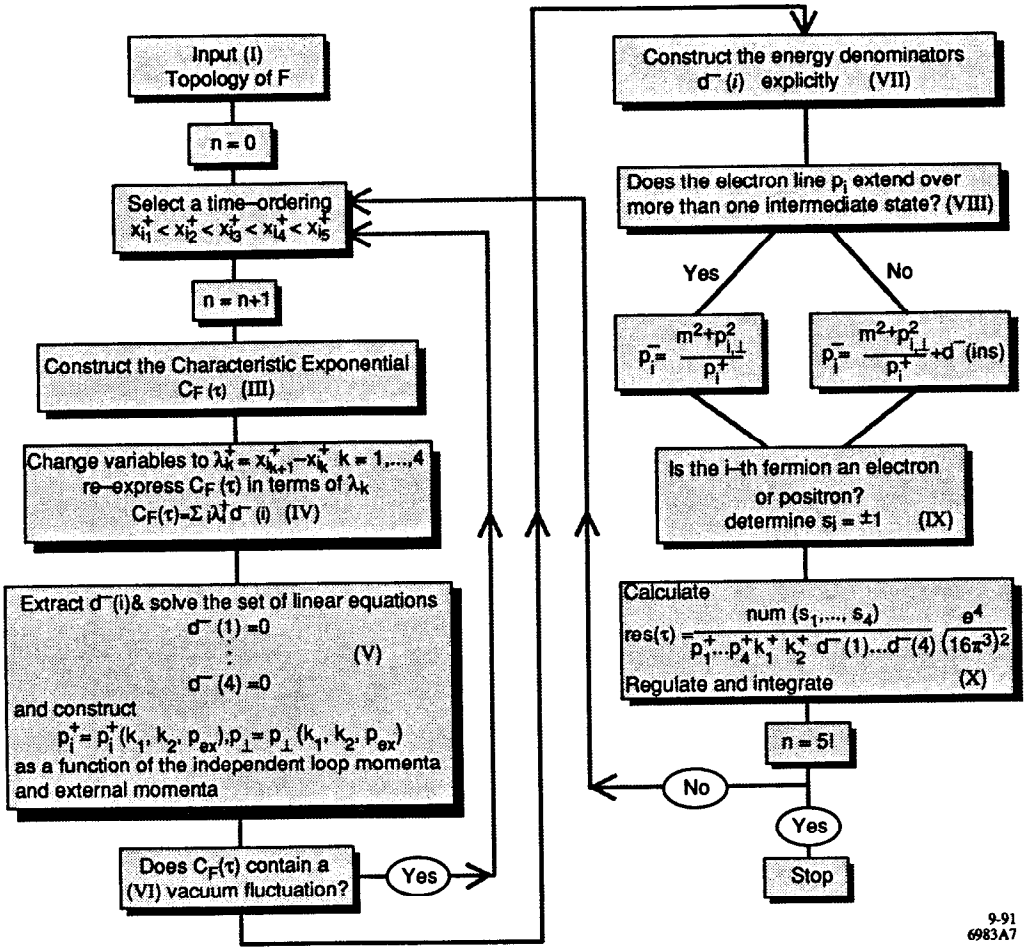
Input (I)
Topology of F
n = 0
Select a time–ordering
$x_{i_1}^+ < x_{i_2}^+ < x_{i_3}^+ < x_{i_4}^+ < x_{i_5}^+$
n = n+1
Construct the Characteristic Exponential
$C_F(\tau)$ (III)
Change variables to $\lambda_k^+ = x_{k+1}^+ - x_k^+$ k = 1,...,4
re–express $C_F(\tau)$ in terms of λ_k
$C_F(\tau) = \Sigma \lambda_i^+ d^-(i)$ (IV)
Extract $d^-(i)$& solve the set of linear equations
$d^-(1) = 0$
:
$d^-(4) = 0$ (V)
and construct
$p_i^+ = p_i^+(k_1, k_2, p_{ex}), p_\perp = p_\perp(k_1, k_2, p_{ex})$
as a function of the independent loop momenta
and external momenta
Does $C_F(\tau)$ contain a
(VI) vacuum fluctuation?
Yes
Construct the energy denominators
$d^-(i)$ explicitly (VII)
Does the electron line p_i extend over
more than one intermediate state? (VIII)
Yes
No
$p_i^- = \frac{m^2+p_{i,\perp}^2}{p_i^+}$
$p_i^- = \frac{m^2+p_{i,\perp}^2}{p_i^+} + d^-(ins)$
Is the i–th fermion an electron
or positron?
determine $s_i = \pm 1$ (IX)
Calculate
$res(\tau) = \frac{num(s_1,...,s_4)}{p_1^+...p_4^+ k_1^+ k_2^+ d^-(1)...d^-(4)} \frac{e^4}{(16\pi^3)^2}$
Regulate and integrate (X)
n = 5!
No
Yes
Stop
9-91
6983A7

Fig. 3

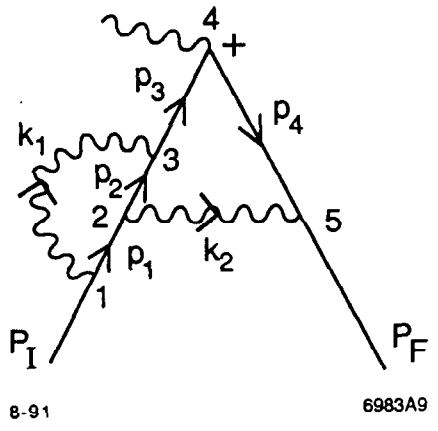

Fig. 4

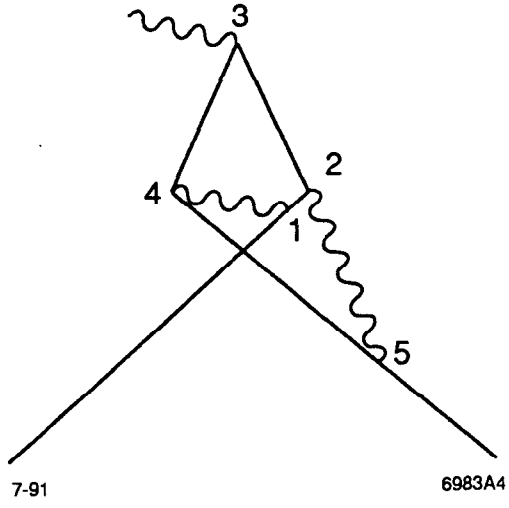

Fig. 5

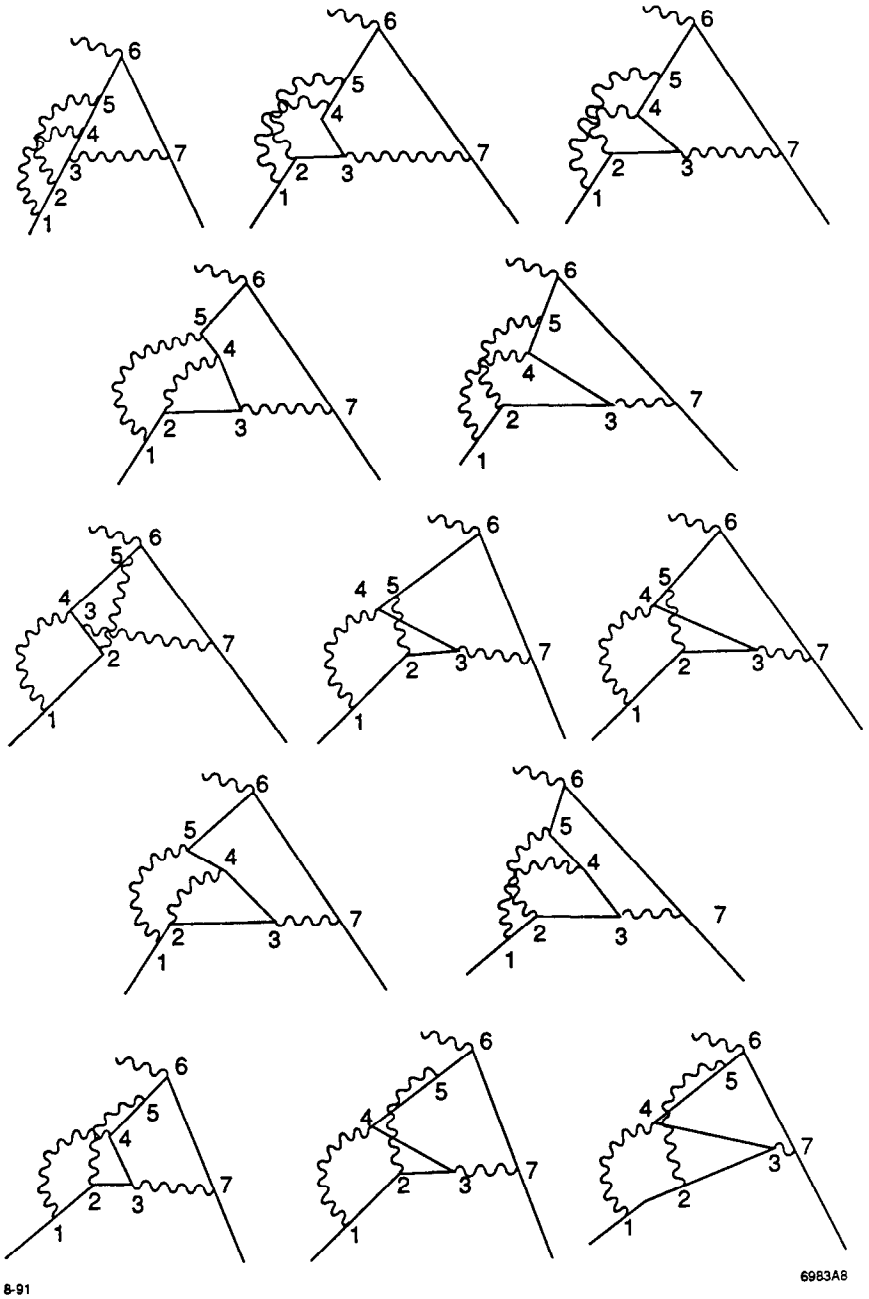

Fig. 6

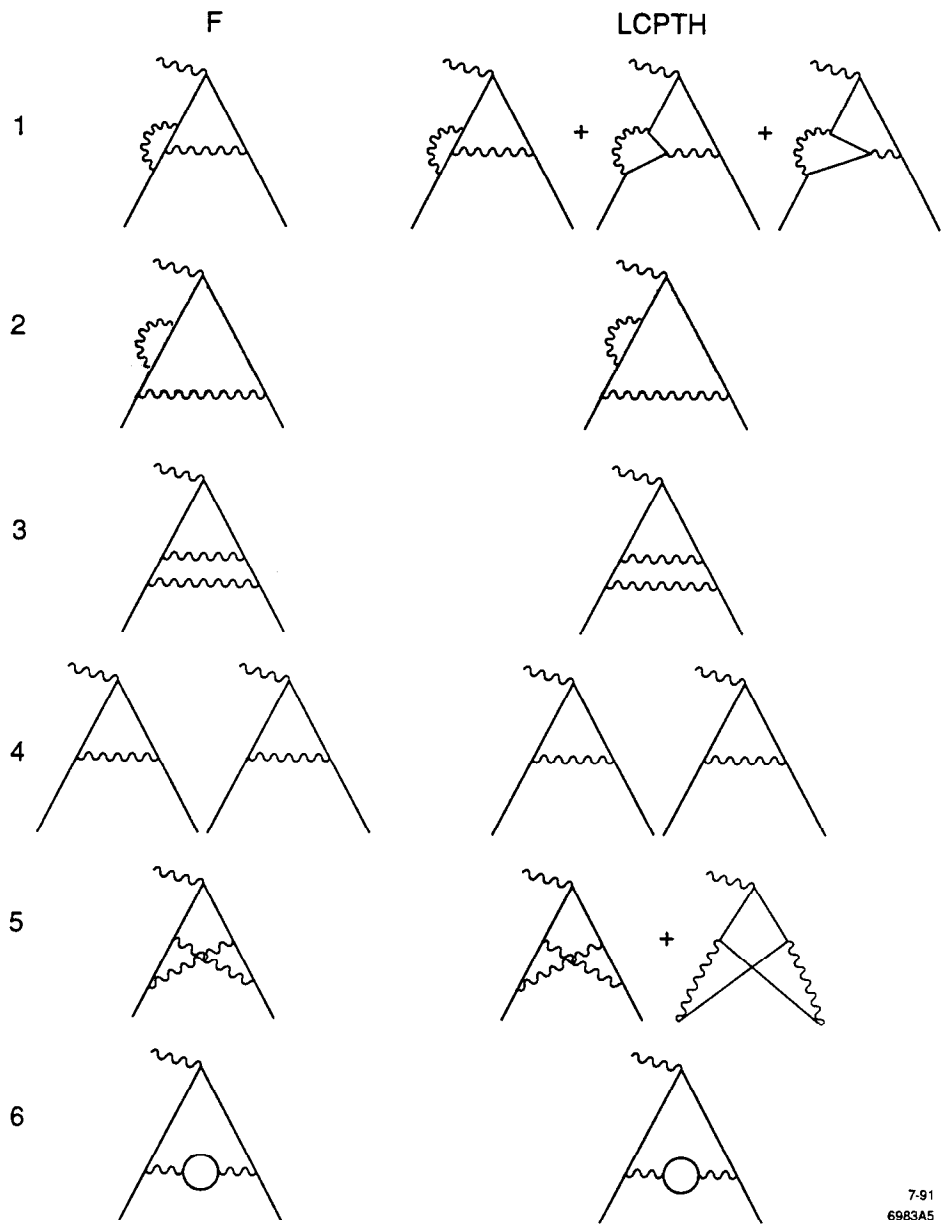

Fig. 7

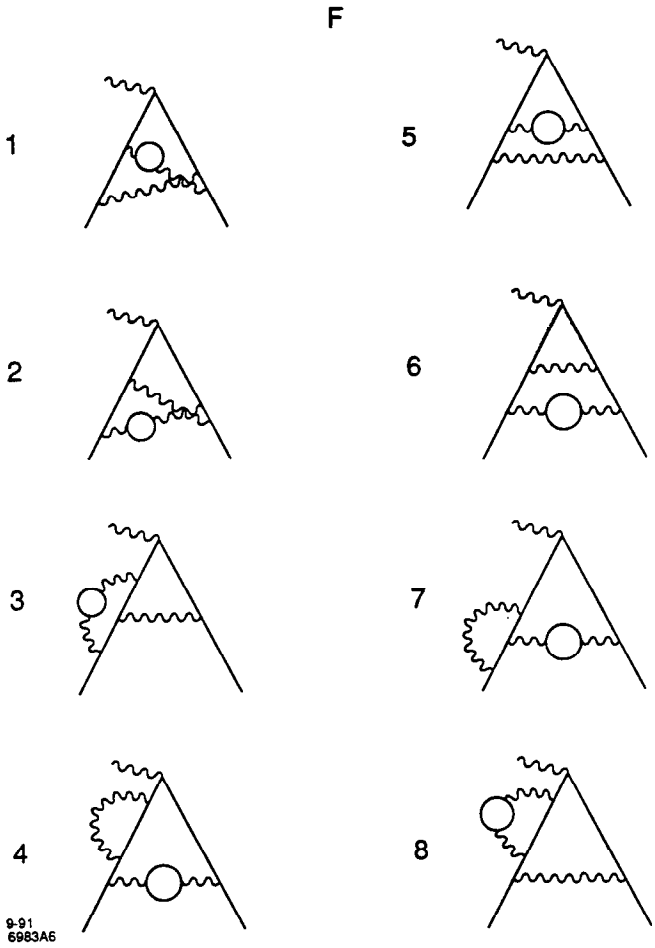

Fig. 8

δa	$Lambda$
-0.289	25
-0.305	50
-0.313	100
-0.324	1000

Table 1

diagram	δa	result by Petermann
1+2	-0.326 ± 0.001	-0.327
3+4	0.780 ± 0.007	0.778
5	-0.465 ± 0.002	-0.467
6	0.016 ± 0.001	0.016

Table 2

diagram	δa	result by Brodsky and Kinoshita
4+7	-0.114 ± 0.002	-0.115
1+2	-0.0031 ± 0.003	-0.0032
5+6	0.053 ± 0.002	0.053
3+8	-0.09 ± 0.02	-0.088

Table 3